UNLIMITED
UNCLASSIFIED

ILLIMITÉ
NON CLASSIFIÉ

Technical Report

Rapport technique

1984/03

TR-WE-41
NRC NO. 23208

CONTACT GEOMETRY BETWEEN WHEEL FLANGE AND RAIL

J. Kalousek

Division of
Mechanical Engineering

Division de
génie mécanique

National Research Council Canada
Conseil national de recherches Canada

Canada

88-04434/

DIVISION OF MECHANICAL ENGINEERING PUBLICATIONS

DM **(Division of Mechanical Engineering Report)**
Scientific and technical information considered important, complete and a lasting contribution to existing knowledge.

TR **(Technical Report)**
Information less broad in scope but a substantial contribution to existing knowledge.

CTR **(Controlled/Classified Technical Report)**
A Technical Report with controlled distribution for national security, proprietary or other reasons.

LM **(Laboratory Memorandum)**
Preliminary or exploratory information with controlled distribution.

CAT **(Calibration Analysis and Test Report)**
Information on minor laboratory projects or services.

PUBLICATIONS DE LA DIVISION DE GÉNIE MÉCANIQUE

DM **(Rapport de la Division de génie mécanique)**
Informations scientifiques et techniques jugées importantes, complètes et susceptibles de contribuer de façon durable à l'avancement des connaissances courantes.

TR **(Rapport technique)**
Informations de moindre importance, mais pouvant contribuer substantiellement à l'avancement des connaissances actuelles.

CTR **(Rapport technique à diffusion contrôlé/classifié)**
Rapport technique à diffusion contrôlée pour des raisons de sécurité nationale, de propriété intellectuelle et autres.

LM **(Mémoire de laboratoire)**
Informations préliminaires ou de nature exploratoire à diffusion contrôlée.

CAT **(Rapport d'étalonnage d'analyse et d'essai)**
Informations sur de petits projets ou des services de laboratoire.

UNLIMITED
UNCLASSIFIED

ILLIMITÉ
NON CLASSIFIÉ

CONTACT GEOMETRY BETWEEN WHEEL FLANGE AND RAIL

GEOMETRIE DE CONTACT ENTRE LE BOUDIN DE LA ROUE ET LE RAIL

J. Kalousek

Division of Mechanical
Engineering Report

Rapport de la Division
de Génie Mécanique

1984/03

TR-WE-41
NRC NO. 23208

Dr. C. Dayson, Head
Division of Mechanical Engineering
Vancouver, B.C., Canada
V6R 1P5

Mr. E.H. Dudgeon
Director/Directeur

ACKNOWLEDGEMENT

This report describes a portion of a broad rail/wheel wear research program which has been undertaken jointly by the Western Laboratory and the University of Rhode Island. The financial support of the Transportation Development Centre (Canada) and the Association of American Railroads towards this program is greatly appreciated. The author also expresses his gratitude to Mr. H. Ackroyd for his excellent technical assistance and to Mrs. K. Fassler for meticulous typing of the manuscript.

ABSTRACT

This report is concerned with contact between the conical section of a wheel flange and the flat portions of the gauge side rail between wheel and straight rail and wheel and disc rail. Experimental observations strongly support the theoretical analyses of contact geometry, slippages and frictional flange force.

RÉSUMÉ

Le contact entre la section conique du boudin d'une roue et la portion plate du côté intérieur d'un rail est décrit pour les cas expérimentaux effectués en laboratoire et sur les rails.

Les observations expérimentales supportent avec force les analyses théoriques de la géométrie du contact, du phénonène de glissement et de la force tangentielle de frottement du boudin de la roue.

NOMENCLATURE

a, b	major and minor semiaxis of flange contact ellipse
e_x, e_z	longitudinal and vertical distance between contact points B and C
h	distance between two mesh points within the contact area
r_c	wheel flange radius at point C
r'_c, r''_c	rail and wheel disc radii at point C
r_{hor}	radius of curvature at point C in a horizontal plane parallel to the wheelset axis
r'_{hor}, r''_{hor}	rail and wheel disc horizontal radii at point C
r_w, r_r	wheel and rail disc radii at contact point B
R', R''	rail and wheel radii normal to contact zone
l, c	subscripts denoting longitudinal and cross-sectional planes normal to contact zone
V_i	slip speed vectors at individual mesh points
α	semiapex angle of wheel flange conical section
β	angle between gauge side of rail and a wheelset axis
γ	angle of wheel's rotation
Δs	length of streak or wear mark left by a wheel asperity on a side of rail
ψ	angle-of-attack (yaw angle of wheelset with respect to track centerline)
ω	angular speed of a wheelset

CONTENTS

		Page
	ACKNOWLEDGEMENT	(ii)
	ABSTRACT	(iii)
	NOMENCLATURE	(iv)
1.0	INTRODUCTION	1
2.0	THEORETICAL CONSIDERATIONS	1
	2.1 Wheel and Straight Rail	1
	2.2 Wheel and Disc Rail	3
3.0	EXPERIMENTAL VERIFICATION OF CONTACT GEOMETRY	4
4.0	SLIPPAGE	4
5.0	FLANGE FRICTION FORCE	6
6.0	CONCLUSIONS	7
	REFERENCES	9

ILLUSTRATIONS

Fig.		
1	Flange Contact Between Wheel and Rail	10
2a	Rail/Wheel Contact Geometries Leading to Elliptical Flange Contacts	11
2b	Radii of Curvature of Normal and Horizontal Conical Sections at C	11
3a	Advancement of Flange Contact Caused by Yaw Misalignment	12
3b	Advancement of Flange Contact for Wheel/Rail Disc Apparatus	12
4	Change in Longitudinal Distance Between Tread and Flange Contact Zones as Function of Angle-of Attack	13
5	Theoretical and Measured Advancement of Flange Contact Point	14
6	Flange Contact Impressions With Varying α and β	15
7	Generation of Prolate Cycloid	16
8	Distribution of Slip Vectors Within the Flange Contact	17
9	Flange Force Vector and Its Orthogonal Components	18

CONTACT GEOMETRY BETWEEN WHEEL FLANGE AND RAIL

1.0 INTRODUCTION

Curving of freight car truck wheelsets can occur in two modes: off-flange and on-flange. During off-flange curving the forces between the wheelset and rails are transmitted through two zones of contact. Though the wheel flange can be in close proximity to the high rail there is no contact. The contact area on the high rail is nevertheless displaced towards the gauge side and is characterized by high conicity. The wheel tread tractions can be determined analytically using the theory of Johnson and Vermeulen [1], sometimes preferred for its simplicity, or by using one of Kalker's several algorithms [2,3], which take more computing time but are more exact. Numerous computer programs have been developed, validated and are currently being used to evaluate the quasi-static or dynamic behaviour of off-flange curving.

During on-flange curving the forces between the wheelset and rails are transmitted through three contact zones: two between the wheel and high rail, and a third between the other wheel and low rail. Although the solutions for the contact zones between wheel treads and rail surfaces are analytically well understood and experimentally validated, the same can not be stated about flange contact. Fortunately, flange contact is less complex than wheel tread/rail surface contact. This is due to the fact that flange contact is subject to sliding only and does not contain any locked-in region as is the case with tread contacts.

This report attempts to summarize the analysis of flange contact including geometry, slip distances and frictional forces. It is hoped that it will benefit those involved in on-flange curving analysis, rolling resistance in curves, wear or derailment studies and simulation of wheel or wheelset behaviour on roller rigs.

2.0 THEORETICAL CONSIDERATIONS

2.1 Wheel and Straight Rail

Hard flange contact occurs between the conical section of the wheel flange profile and the gauge side of the rail. The conical section is typically 7 mm (≈ 1/4") wide on new wheels. This width can increase with wear up to 30 mm (1 1/4"). The flange cone angle, α, also increases with wear from 70° up to over 80°. The flange cone contacts the upper gauge corner of the rail, if it is new, or the flat section of the gauge side of the rail, if it is worn. Thus the problem of flange contact can be reduced to the study of contact between conical and flat surfaces as shown in Figure 1.

The height of the contact point, e_z, is determined from the geometry of the wheelset contacting a pair of rails. To do this, it is necessary to consider not only the shape of rail and wheel profiles but also their mutual orientation. The value, e_z, reaches its maximum when the inclination of the gauge side plane, β, is smaller than the cone angle, α, as shown in Figure 2a. For $\alpha < \beta$ the e_z reaches its minimum and the contact occurs in the vicinity of the flange root.

$\alpha = \beta$ yields a line contact typical of a conical section contacting a flat plane. The length of this contact is, however, severely limited by the lesser height of either the rail's gauge side or the wheel's conical surfaces. The e_z in this case should be measured with respect to the centre of this line contact.

The forward displacement of the flange contact point, e_x, can be determined as a function of the angle-of-attack. Sectioning the flange cone in a horizontal plane yields a parabola of radius of curvature, r_{hor}, at its vertex (see Figure 2b) which is given by the equation:

$$r_{hor} = r_c \, tg\alpha \tag{1}$$

Rolling the vertex of this parabola over the straight side of a rail by a small angle-of-attack, ψ, will yield the displacement of contact point, C, (See Figure 3a), by an amount calculated as follows:

$$e_x = r_{hor} \sin\psi = r_c tg\alpha \sin\psi \tag{2}$$

This relationship was first derived by Bodecker [4] and has been used since by many scientists [5 - 8]. It should be pointed out that the worn flanges, say with $\alpha = 78°$, will result in larger e_x than new wheels with $\alpha = 70°$, due to an increase in r_{hor}. For the 38" diameter wheel this increase amounts to 71%.

The quantities, e_x and e_z, determine the location of the contact point, which becomes the centre of the contact ellipse or the line contact. The dimensions of the contact ellipse or the appropriate section of the line contact are governed by the geometry of the flange and the gauge side of the rail in the immediate vicinity of the contact point. Knowing load and material properties of rail and wheel steels, these dimensions can be calculated using Hertz' theory [9,10]. For the case of $\alpha > \beta$ (See Figure 2a, b) the principal radii are:

$$R''_1 = r_c \sec\alpha; \quad R''_c; \quad R'_1 = \infty; \quad R'_c = \infty \tag{3}$$

For the case $\beta > \alpha$, the principal radii are:

$$R''_1 = r_c \sec\alpha; \quad R''_c = \infty; \quad R'_1 = \infty; \quad R'_c \tag{4}$$

where the values of R''_c and R'_c are determined from the cross-sections of respective rail and wheel profiles under consideration. Since R''_c and R'_c cannot attain large values, the contact ellipse for $\alpha \neq \beta$ will always be rather narrow with its large axis oriented in the longitudinal direction. Such a narrow contact ellipse exhibits small contact area and high contact pressures with a maximum in the range of 500,000 to 800,000 psi.

The line contact geometry at $\alpha = \beta$ is calculated from Hertzian theory applicable to cylindrical contacts [11] taking

$$R''_1 = r_c \sec\alpha \quad \text{and} \quad R'_1 = \infty \tag{5}$$

Since the length of this contact is limited by the lesser height of the gauge side plane or flange cone it could be appreciably smaller than the contact width. Since the cylindrical contacts generally exhibit larger contact areas than elliptical flange contacts, the contact pressures are appreciably reduced, but can still be high enough to bring about a severe form of adhesive wear.

2.2 Wheel and Disc Rail

In many small or full-scale laboratory studies of rail/wheel contact phenomena, the rails are simulated by discs. In order to compare the flange contact data generated in the field with those generated on the disc-on-disc simulator it is necessary to know the distance, e_z and e_x, in both situations.

The vertical depression of the flange contact point, e_z, is determined in the same manner as in the wheel, straight rail situation. The advancement of the contact point, e_x, is generated by rolling the parabola vertexes of the appropriate conical wheel and rail disc sections over each other by a small angle, ψ, as indicated in Figure 3b, i.e.:

$$e_x = \frac{r'_{hor}}{r'_{hor} + r''_{hor}} \quad e_{xo} = \frac{r'_{hor}\, r''_{hor}}{r'_{hor} + r''_{hor}} \sin\psi \tag{6}$$

For most of the experiments carried out on the disc-on-disc simulator, the rail and wheel discs, unless changed frequently, wear into similar, highly conformal profiles. In particular, the slope of the gauge side of the high rail and wheel flange cone angle will be the same i.e. $\alpha = \beta$ and Equation 6 can be written in the form:

$$e_x = \frac{r'_c \cdot r''_c}{r'_c + r''_c} \operatorname{tg}\alpha \sin\psi \tag{7}$$

Comparison of Equations (2) and (7) indicates that for the same values of α and ψ the disc-on-disc simulation will always generate a shorter e_x than the field situation.

The shape of the contact area is again a segment of a line contact connecting the apexes of the wheel flange and gauge side cones. The principal radii of this cylindrical contact are:

$$R'_1 = r'_c \sec\alpha \quad \text{and} \quad R''_1 = r''_c \sec\alpha \tag{8}$$

Hertz' theory which is applicable to line contacts may be used to determine the size and distribution of contact pressure within the flange contact area.

3.0 EXPERIMENTAL VERIFICATION OF CONTACT GEOMETRY

Using a one tenth scale rail/wheel wear apparatus [12], the contact patches were obtained from tread and flange contacts for both wheel and straight rail as well as wheel and disc rail combinations. New and worn profiles were NC machined onto wheel discs, rail discs and straight segments of rail blanks. These were then polished to yield a clearer resolution of the shape and dimensions of contact patch. Aluminum foil was inserted in the rail/wheel interface and then the discs were loaded. After the impressions were taken, the foil was flattened and the impressions were measured. An example of the impressions for angles-of-attack where ψ = 0°0', 0°30', 1° and 2°, using a wheel with CN 'Profile A' and a straight rail containing new AREA profile, are shown in Figure 4. The tread contact areas are ellipses with an a/b ratio close to one. The a/b ratio for flange contact is in the vicinity of 10.

The distance e_x measured between the centres of the tread and flange contact zones for wheel/straight rail and wheel/disc rail combinations was plotted against the angle-of-attack as shown in Figure 5. In general, good agreement was obtained between calculated and measured values. An exception can be observed between ψ = 0 - 36' in the case of flange contact with straight rail. Apparently the gauge corner of the rail was not touching the conical section of the flange but the flange root adjacent to it, i.e. the condition of $R'_c = \infty$ was not satisfied.

The imprints shown in Figures 6a and 6b were taken with $\alpha > \beta$ and $\alpha < \beta$ respectively. The location of the gauge corner in both cases is indicated by the dotted line. Although the distance from the dotted lines to the center of the flange contact zone does not represent the e_z, it does indicate the difference between the two cases considered. Figures 6c and d show the impressions generated by cylindrical flange contact, i.e. when $\alpha = \beta$. The impressions shown in 6c were obtained by using polished disc and straight rail and those shown in 6d were made by using worn wheel and rail discs. Both impressions demonstrate that while the width of the cylindrical contact zone may be appreciable, its length is limited by the size of the conical section of the wheel flange or the flat portion of the gauge side of the rail.

4.0 SLIPPAGE

Knowledge of slip vector distribution throughout the contact zone leads to a better understanding of friction and wear processes, rolling resistance and generation of frictional force within flange contact.

Providing the wheel does not slip at point G in a longitudinal direction, point C on the wheel flange will follow the trajectory of a prolate cycloid. Although we are interested only in that portion of the point C trajectory which lies below the rail's top surface, the manner by which the entire prolate cycloid is generated is shown in Figure 7. Analytically, the curve is described by the following parametric equations:

$$x = r_w\gamma - r_c\sin\gamma$$
$$z = r_w - r_c\cos\gamma \qquad (9)$$

Any prolate cycloid or its portion is easily drawn by using the following rule: A line, connecting the generating point C with contact point G, is always normal or perpendicular to the tangent at point C. The tangent itself indicates the instantaneous direction of a velocity vector. When point C is in contact with the gauge side of the rail, the tangent to C also indicates the direction of the slip vector with respect to the rail.

Letting the generating circle roll by an incremental angle of, say, $\Delta\gamma$, it is possible to plot the instantaneous values of slip vectors for a few selected flange contacts. Three examples of slip vectors within the flange contact are shown in Figure 8. Figure 8a shows the slip vectors for the case in which $\alpha > \beta$ and $\psi = 0$. Although flange contact at $\psi = 0$ rarely occurs in the field because it requires large, unbalanced speeds, this case clearly demonstrates that the instantaneous slip vectors within the flange contact are always symmetrical about the centre of the contact ellipse, i.e. point C. The same observation can be made for the other two cases (Figures 8, b & c) which are, of course, more typical examples of contact geometry occuring in the field than case (a). Providing the distance, h, between the two mesh points within the contact ellipse is $h = r_c\sin\Delta\gamma$, we can construct the shape and length of a slip mark or streak left on a side of rail by a wheel asperity by summing up the instantaneous slip vectors along the ellipse's longitudinal axis. Close agreement was obtained between streaks actually observed and those acquired by the above method. Inset photographs in Figure 8 depict the actual slip marks on the gauge side of a rail corresponding to the discussed cases.

The radius of curvature of a streak can be determined analytically using the following formula:

$$R_s = \frac{[r_w^2 - 2r_w r_c\cos\gamma + r_c^2]^{3/2}}{r_w r_c\cos\gamma - r_c^2} \qquad (10)$$

$$\text{where } \gamma = \arcsin\frac{e_x}{r_c}$$

The streak length is constrained by either the width of the contact ellipse, 2b, or the length of the cylindrical contact, 2a. Thus:

$$\Delta s = 2b \text{ (ellipse)}$$
$$= \frac{2a\sqrt{e_x^2 + e_y^2}}{r_w\sin\alpha} \text{ (cylindrical contact)} \qquad (11)$$

Since the contact pressures at the edges of elliptical or cylindrical contact zones may be insufficient to produce plastic deformation of a substrate layer of metal, a more realistic estimate of slip distance is obtained when right-hand expressions in Equation 11 are multiplied by 2/3.

The typical slip length values for hard flange contacts, either calculated or measured, lie in the vicinity of 2.5 mm (0.1"). Depending on the misalignments of a particular wheelset the average slip distance in flange contact may be twenty to several hundred times larger than the average slip in tread contact. The unusually large wear rates observed on wheel flanges and sides of high rails in curves must therefore be attributed to long flange contact slip distances which, on the average, are two orders of magnitude larger than those occuring in tread contact.

In a disc-on-disc configuration the trajectory of a wheel asperity with respect to the rail disc is a prolate epicycloid. The same rule which applies to the design of cycloids governs the generation of epicycloids. The parametric equations of a prolate epicycloid are:

$$x = (r_w + r_r)\cos\gamma - r_c\cos\frac{r_w + r_r}{r_w}\gamma \qquad (12)$$

$$z = (r_w + r_r)\sin\gamma - r_c\sin\frac{r_w + r_r}{r_w}\gamma$$

Within the area of flange contact the prolate epicycloid will always exhibit larger curvature than the prolate cycloid. This curvature increases with the decreasing diameter of rail discs. The slip distances may be estimated using Equation 11. Due to a smaller e_x value these become somewhat shorter than those occuring in a wheel, straight rail flange contact, but the flange-tread slip distance ratio still lies in the two order of magnitude range.

5.0 FLANGE FRICTION FORCE

The magnitude of friction force in flange contact is given by a product of the friction coefficient and the magnitude of a normal load, and lies in the direction of rubbing or slippage. The load at the flange contact is dependent on a number of parameters, including tread forces at both wheels, external loading environment and truck suspension. As a rule computer programs or measurements are used to arrive at a good estimate of flange loading. In some instances it can reach a value exceeding that of a vertical wheel load.

The only place at which unsaturated or zero slippage could be obtained is at point B where $e_x = e_z = 0$. Because all flange contact points have $e_z > 0$, the flange contact area will always experience saturated slippage. In other words, no portion of the flange contact area, however small, can contain a locked in region in which the

rail and wheel asperities do not move with respect to each other. However, at different locations within the contact zone, asperities will move at different speeds with respect to their underlying rail points. This speed increases with the distance from point B according to the following formula:

$$V_i = \omega\sqrt{e^2_{xi} + e^2_{zi}} \quad i = 1,..,n \tag{13}$$

Thus the rubbing speed of flange asperities is, by a factor of about 15 to 60, smaller than the speed of the train or the wheel's flange periferal speed. The range of rubbing speeds experienced by flange asperities is not sufficiently large enough to affect the value of the coefficient of friction. Therefore, each asperity, whether near or far from B, produces equal friction force under the same contact pressure. Considering the symmetry of contact pressure and the direction of slip vectors with respect to point C, it follows that the direction of a resultant vector obtained by summing up all frictional forces produced by individual asperities (or, equivalently, summing up all traction forces produced within the discretised subregions of the contact area) must be coincident with the slip direction at point C. Therefore the direction of the slip vector at point C is the exact rather than an approximate estimate of the flange force direction. Unfortunately, the magnitude of this force can only be determined as accurately as the estimate of the coefficient of friction. The friction coefficient could change anywhere from 0.05 for well lubricated contacts and smooth surfaces; to 0.3 for contacts experiencing mild adhesive wear; to 0.6 for contacts experiencing gouging wear.

Decomposing the flange force (L) into its orthogonal components, as shown in Figure 9, it can be seen that this force resists the wheel's rotation, L_x, increases the flange loading, L_y, and unloads the wheel/rail contact point B, L_z. The unloading of contact point B is less pronounced in disc-on-disc rail/wheel simulators, for otherwise identical misalignments and external loading environments, than in the field situation. This is caused by the distance, e_x, which is always shorter in disc-on-disc than wheel on straight rail arrangements. For the same reason the flange contact in disc-on-disc simulators generates larger rotational resistance than the equivalent field situation. The amount of decrease in wheel unloading or increase in rotational resistance can easily be evaluated if the e_x and e_z values are known for both disc-on-disc and field situations.

6.0 CONCLUSIONS

The purpose of this report has been to present a brief, but concise, analysis of flange contact as it occurs between wheels and rails and wheels and discs using simulating apparatuses. It has been shown that:

(1) The flange contact area is either a narrow ellipse oriented in a longitudinal direction, or a cylindrical contact of short length. Its location with respect to tread contact is given by longitudinal and vertical coordinates, e_x and e_z. Hertz' theory must be used to determine the ellipse dimensions.

(ii) The slip directions within the zone of contact are determined by the e_{xi} and e_{zi} coordinates of an individual mesh point. The directions and magnitudes of slip vectors are symmetrical with respect to point C.

(iii) The flange force, always generated by saturated slip, takes on the direction of the slip vector at point C. Its magnitude is determined by the magnitude of force normal to the flange contact and rheological environment, prevailing in the flange contact area.

REFERENCES

1. Johnson, K.L. Vermeulen, P.J. "Contact of Non-Spherical Bodies Transmitting Tangential Forces". Journal of Applied Mechanics, June 1964.

2. Kalker, J.J. "Simplified Theory of Rolling Contact". Delft Progress Report, Ser. C,1, 1-10, 1973.

3. Kalker, J.J. "Introduction to the Fortran IV Programs DUVOROL and CONTACT for the Solution of 3-D Elastostatic Half-Space Contact Problems With or Without Friction". Delft University of Technology, Dept. of Mathematics, Report 82-29, 1982.

4. Bodecker, C. "Die Wirkung Zwischer Rad und Schiene". 1887.

5. Muller, C.T. "The Railway Wheelset, Kinematics, Geometry of Track Guidance, Guiding Capacity". Glasers Annln, Sept. 1953.

6. Matsui, N. "On the Derailment Quotient Q/P'". Railway Technical Research Institute, Japanase National Railways, 1966.

7. Gilchrist, A.O. Brickle, B.V. "A Re-examination of the Proneness to Derailment of a Railway Wheelset". J. Mech. Eng. Sci., Vol. 18, No. 3, pp. 131-141, 1976.

8. Marcotte, P.P. Matheson, K.J.R. Young, R. "A Practical Model of Rail Vehicle Curve Negotiation". Proceedings of the 7th Symposium of the International Association for Vehicle System Dynamics, Cambridge, 1981.

9. Hoersch, V.A. Thomas, H.R. "Stresses Due to the Pressure of One Elastic Solid Upon Another". University of Illinois Bulletin, Vol. 27, No. 24, 1930.

10. Seely, F.B. Smith, J.O. "Advanced Mechanics of Materials". Wiley, pp. 342-378, 1952.

11. Timoshenko, S.P. Goodier, J.N. "Theory of Elasticity". McGraw Hill, 1970.

12. Kalousek, J. "Rail/Wheel Wear Testing Facility". NRCC Newsletter on Transportation, Vol. 13, No. 1, July 1981.

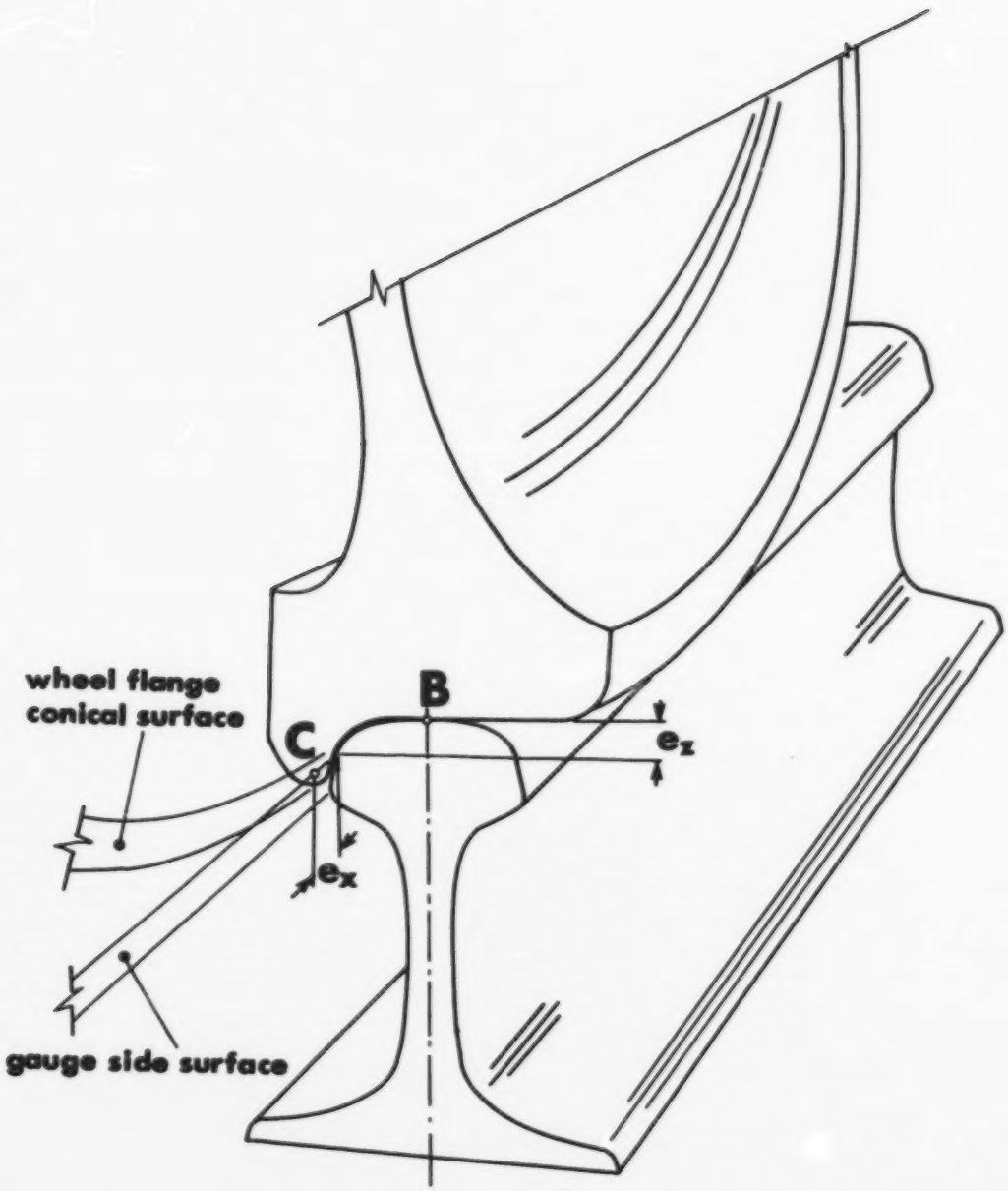

FIGURE 1: Flange Contact Between Wheel and Rail

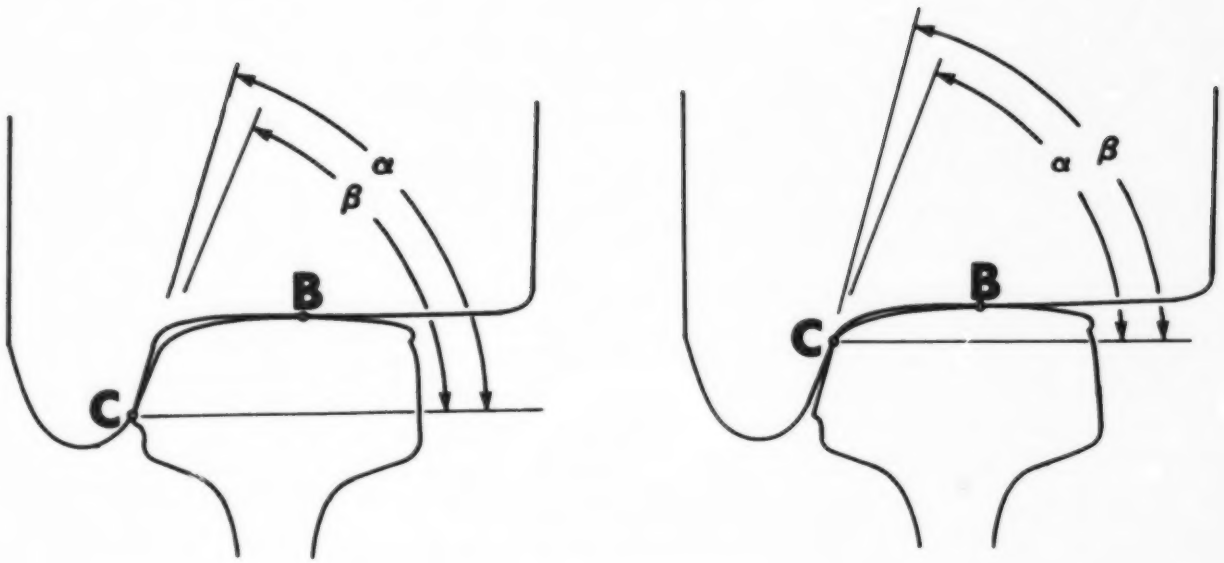

a) Rail/Wheel Contact Geometries Leading To Elliptical Flange Contacts

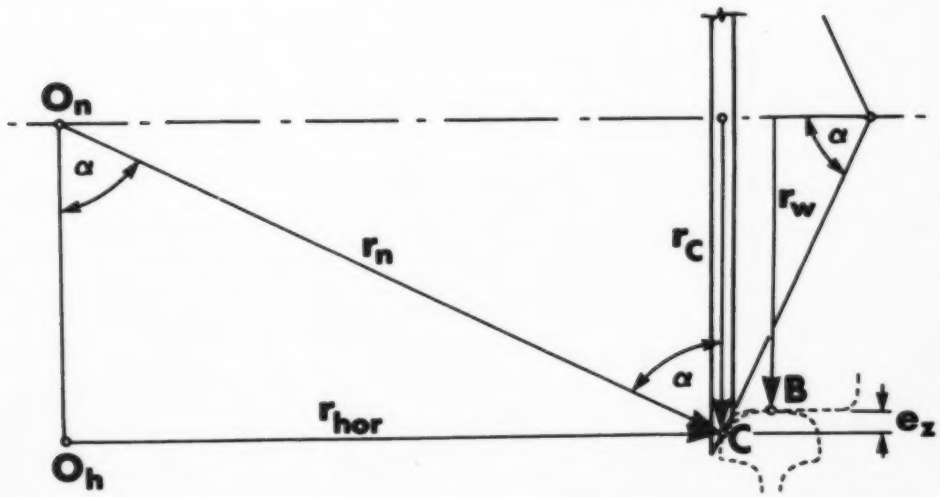

b) Radii of Curvature of Normal and Horizontal Conical Sections at C

FIGURE 2

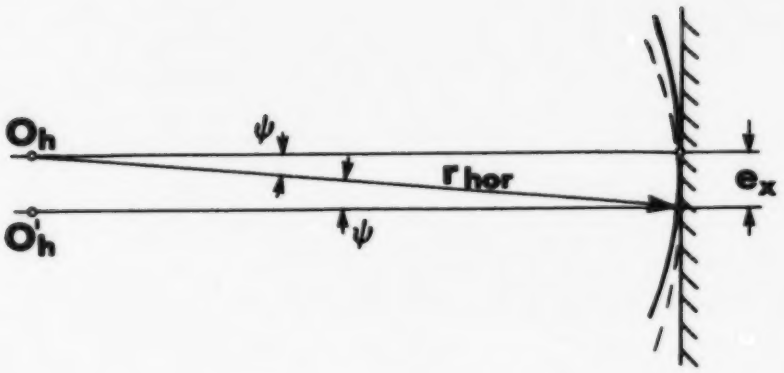

a) Advancement of Flange Contact Caused by Yaw Misalignment of a Wheelset

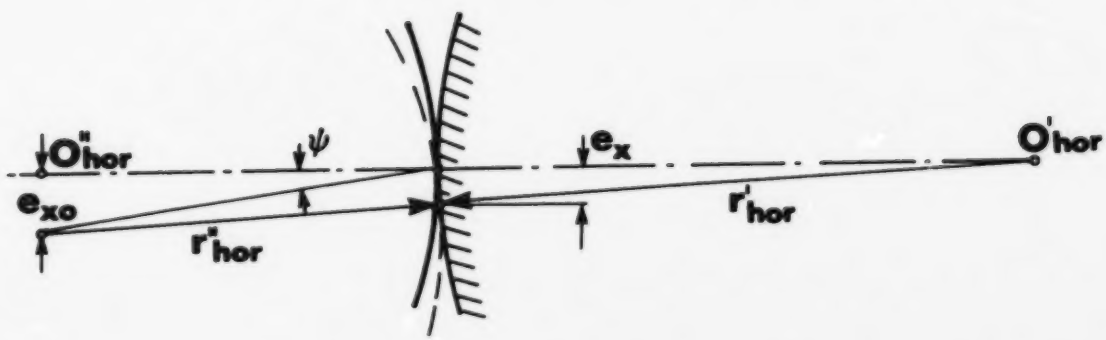

b) Advancement of Flange Contact for Wheel/Rail Disc Apparatuses

FIGURE 3

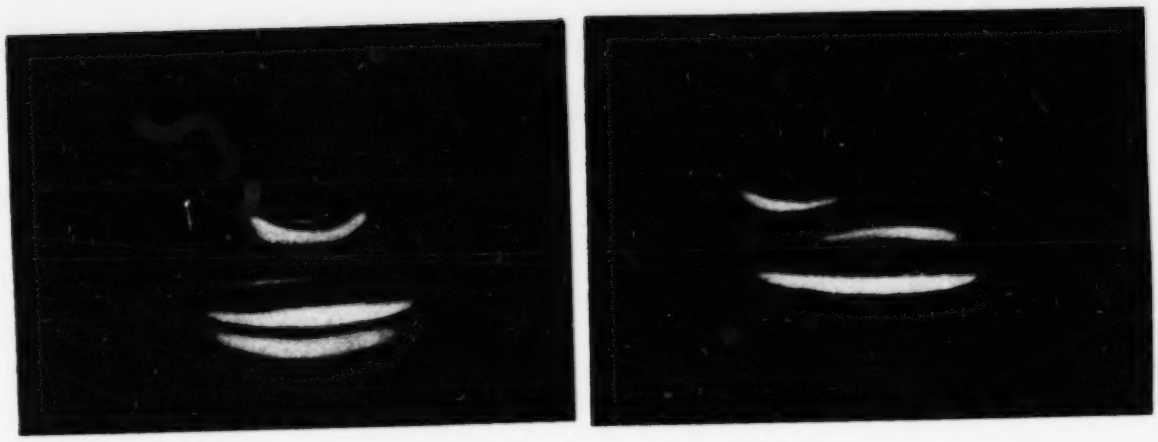

a) $\psi = 0$

b) $\psi = 30'$

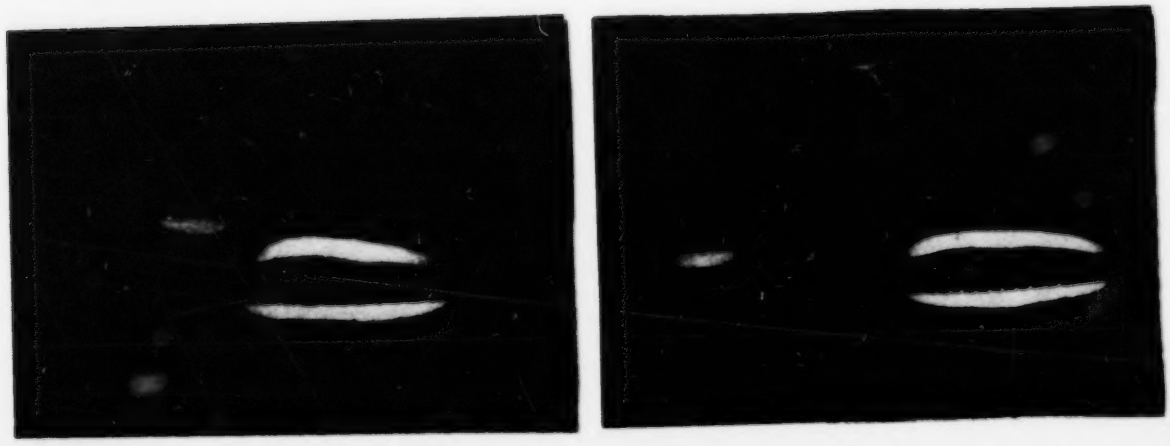

c) $\psi = 60'$

d) $\psi = 120'$

FIGURE 4: Change in Longitudinal Distance Between Tread and Flange Contact Zones as Function of Angle-of-Attack

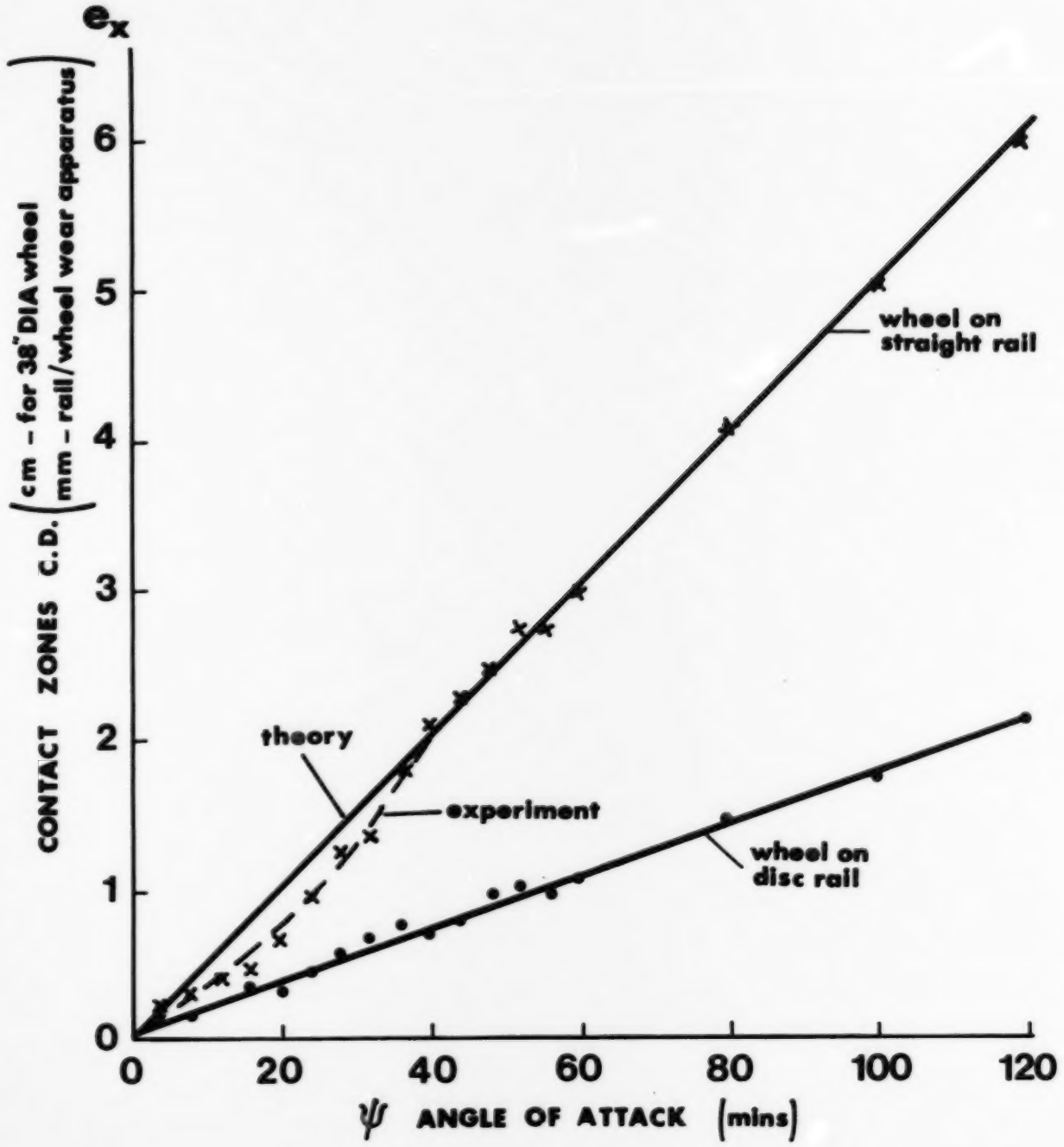

FIGURE 5: Theoretical and Measured Advancement of Flange Contact Point

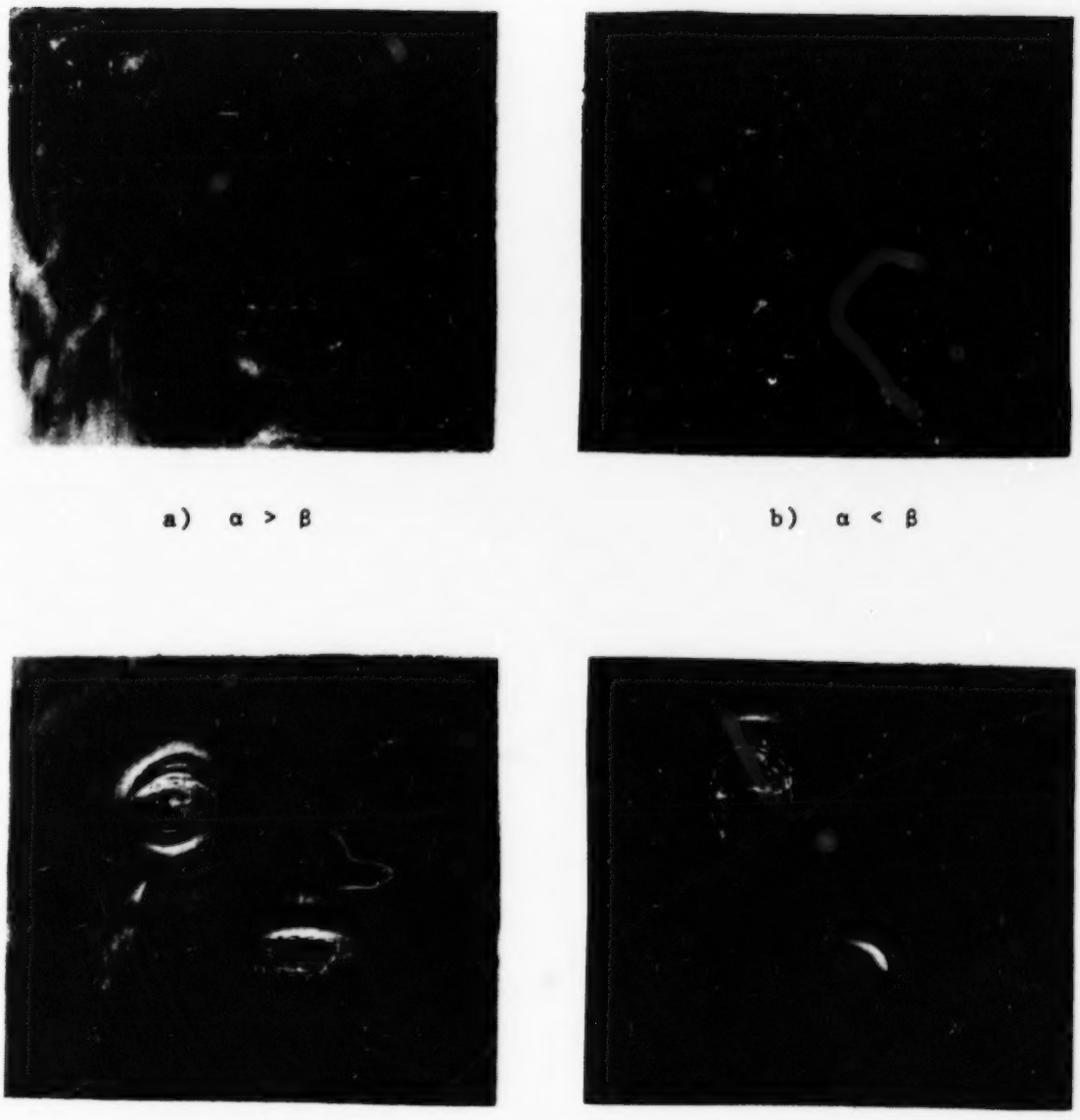

a) $\alpha > \beta$

b) $\alpha < \beta$

c) $\alpha = \beta$

d) $\alpha = \beta$

FIGURE 6: Flange Contact Impressions With Varying α and β

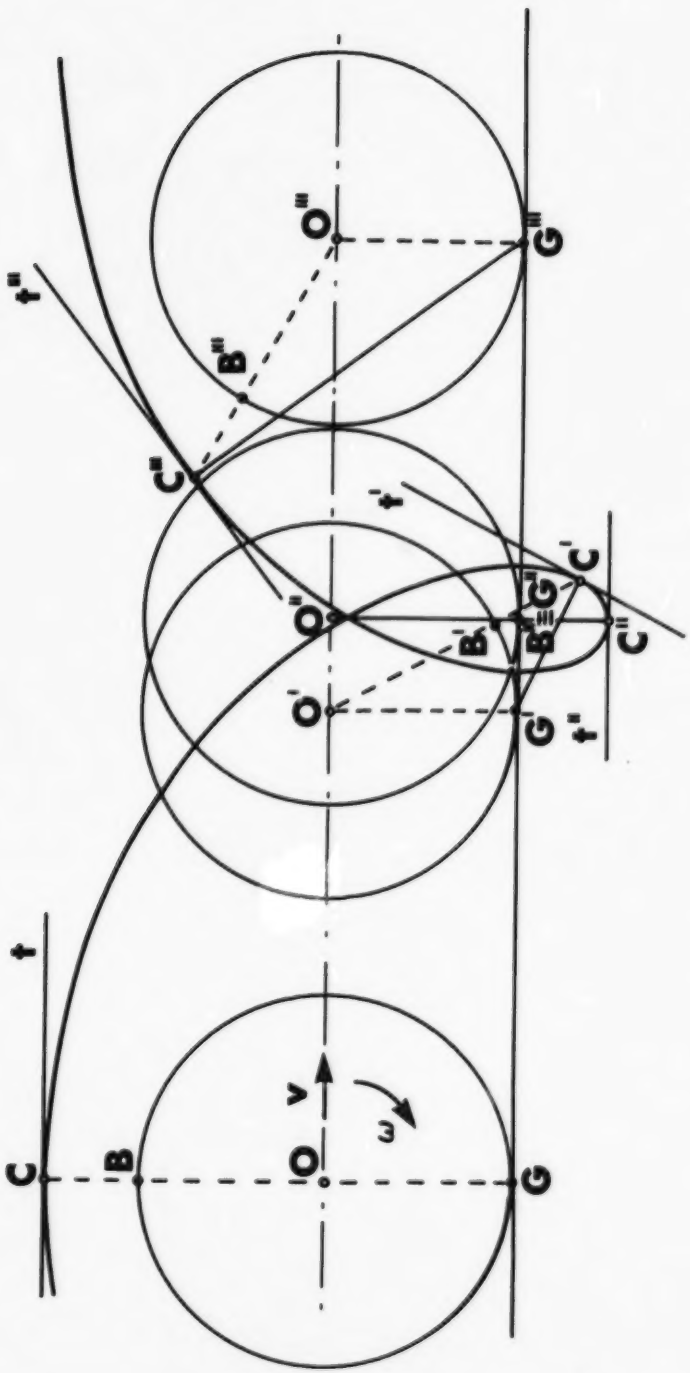

FIGURE 7: Generation of Prolate Cycloid

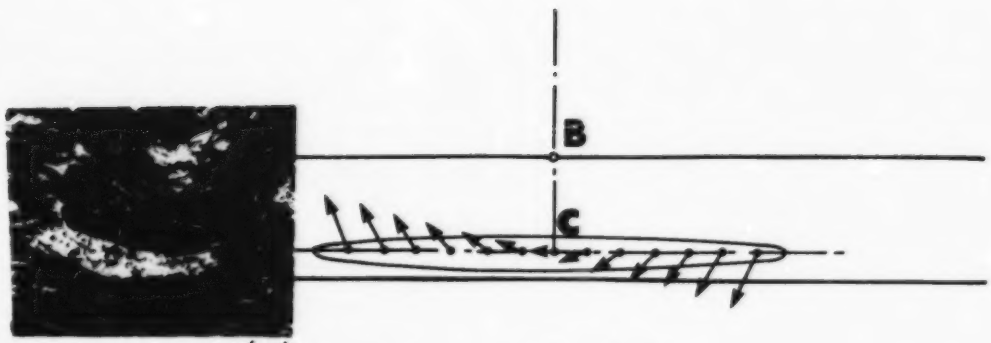

(a) $\alpha > \beta$, ψ = zero

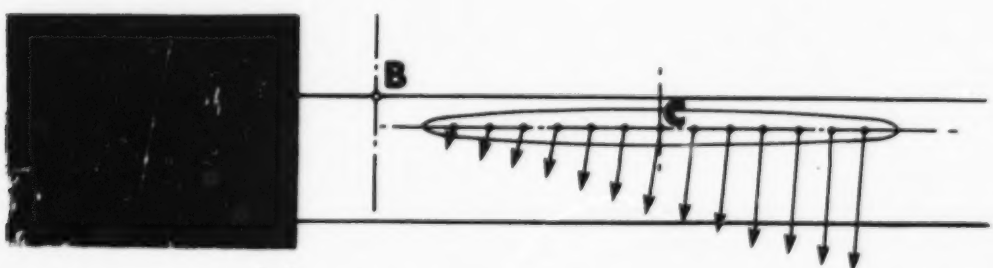

(b) $\alpha < \beta$, large ψ

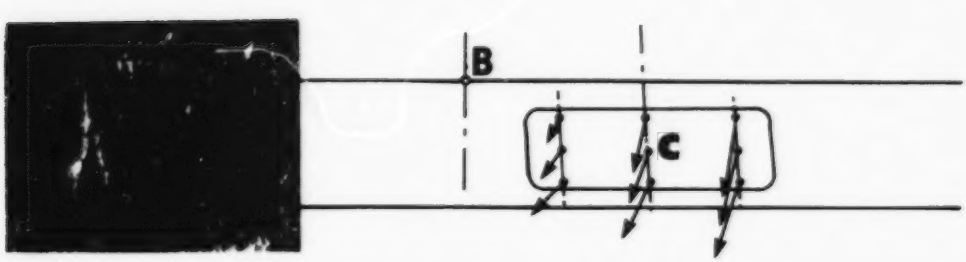

(c) $\alpha = \beta$, moderate ψ

FIGURE 8: Distribution of Slip Vectors Within the Flange Contact

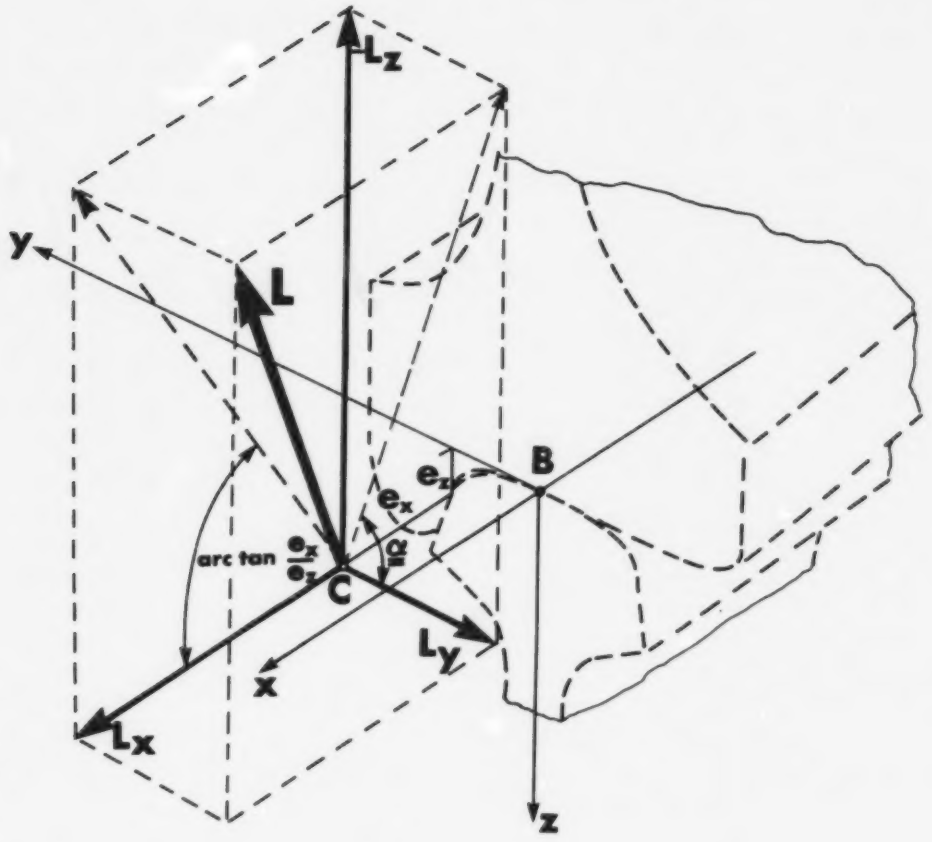

FIGURE 9: Flange Force Vector and Its Orthogonal Components

REPORT DOCUMENTATION PAGE/PAGE DE DOCUMENTATION DE RAPPORT

REPORT/RAPPORT	REPORT/RAPPORT
1a TR-WE-41	1b
REPORT SECURITY CLASSIFICATION CLASSIFICATION DE SÉCURITÉ DE RAPPORT	DISTRIBUTION/DIFFUSION
2 UNCLASSIFIED	3 UNLIMITED

TITLE/SUBTITLE/TITRE/SOUS-TITRE (CLASSIFICATION)

4 CONTACT GEOMETRY BETWEEN WHEEL FLANGE AND RAIL (UNCLASSIFIED)

AUTHOR(S)/AUTEUR(S)

5 J. Kalousek

SERIES/SÉRIE

6 Technical Report

CORPORATE AUTHOR/PERFORMING AGENCY/AUTEUR D'ENTREPRISE/AGENCE D'EXÉCUTION

7 National Research Council Canada (Western Laboratory)
Division of Mechanical Engineering

SPONSORING AGENCY/AGENCE DE SUBVENTION

8 Transport Canada, Transportation Development Centre,
1000 Sherbrooke St. W., Montreal, Quebec H3A 2R3

DATE	FILE/DOSSIER	LAB. ORDER COMMANDE DU LAB.	PAGES	DIAGS	REFS
9 1984/03	10 3793-2-4	11 22200	12a 18	12b 11	12c 1

NOTES

13

DESCRIPTORS(KEY WORDS)/MOTS-CLÉS

14 Geometry of Flange Contact, Wheel Flange, Side Wear of Rails, Rail/Wheel Creepages, Rail/Wheel Forces

SUMMARY/SOMMAIRE

15 Contact between the conical section of a wheel flange and the flat portion of the gauge side of rail is described for the cases of wheel and straight rail and wheel and disc rail.

ADDRESS/ADRESSE

16 Dr. C. Dayson (Head)
Western Laboratory
3904 West 4th Avenue
Vancouver, B.C. V6R 1P5 (604) 732-4477